Journal of Macromolecular Science, Part A
Publication details, including instructions for authors and subscription information:
http://www.informaworld.com/smpp/title~content=t713597274

Modeling of the Homogeneous Free-Radical Copolymerization Kinetics of Fluoromonomers in Carbon Dioxide at Supercritical Conditions

Iraís A. Quintero-Ortega[ab]; Eduardo Vivaldo-Lima[ac]; Ram B. Gupta[b]; Gabriel Luna-BáRcenas[d]; Alexander Penlidis[c]
[a] Departamento de Ingeniería Química, Facultad de Química, Universidad Nacional Autónoma de México (UNAM), México, D.F., México [b] Department of Chemical Engineering, Auburn University, Auburn, Alabama [c] Institute for Polymer Research (IPR), Department of Chemical Engineering, University of Waterloo, Waterloo, Ontario, Canada [d] CINVESTAV, Unidad Querétaro, Querétaro, México

To cite this Article Quintero-Ortega, Iraís A. , Vivaldo-Lima, Eduardo , Gupta, Ram B. , Luna-BáRcenas, Gabriel and Penlidis, Alexander(2007) 'Modeling of the Homogeneous Free-Radical Copolymerization Kinetics of Fluoromonomers in Carbon Dioxide at Supercritical Conditions', Journal of Macromolecular Science, Part A, 44: 2, 205 — 213
To link to this Article: DOI: 10.1080/10601320601031374
URL: http://dx.doi.org/10.1080/10601320601031374

Journal of Macromolecular Science®, Part A: Pure and Applied Chemistry (2007) **44**, 205–213

ISSN: 1060-1325 print/1520-5738 online
DOI: 10.1080/10601320601031374

Modeling of the Homogeneous Free-Radical Copolymerization Kinetics of Fluoromonomers in Carbon Dioxide at Supercritical Conditions

IRAÍS A. QUINTERO-ORTEGA,[1,2] EDUARDO VIVALDO-LIMA,[1,3,†] RAM B. GUPTA,[2] GABRIEL LUNA-BÁRCENAS,[4] and ALEXANDER PENLIDIS[3]

[1]*Departamento de Ingeniería Química, Facultad de Química, Universidad Nacional Autónoma de México (UNAM), México, D.F., México*
[2]*Department of Chemical Engineering, Auburn University, Auburn, Alabama*
[3]*Institute for Polymer Research (IPR), Department of Chemical Engineering, University of Waterloo, Waterloo, Ontario, Canada*
[4]*CINVESTAV, Unidad Querétaro, #2000, Real de Juriquilla, Frac, Querétaro, México*

Received and accepted August, 2006

Simulations of the free-radical homopolymerization and copolymerization kinetics of fluoromonomers in carbon dioxide at supercritical conditions are presented. The homogeneous homopolymerization of dihydroperfluorooctyl acrylate (FOA) and the surfactant-free precipitation copolymerization of tetrafluoroethylene (TFE) with vinyl acetate (VAc) in supercritical carbon dioxide were used as case studies. Reasonable agreement between experimental data from the literature and model predictions of monomer conversion vs. time, number and weight average molecular weights vs. conversion, and copolymer composition vs. conversion, for the above mentioned systems, was obtained.

Keywords: supercritical carbon dioxide; homogeneous polymerization; copolymerization; modeling; fluoropolymers

1 Introduction

Fluoropolymers are typically synthesized in aqueous polymerization systems (both emulsion and suspension), non-aqueous systems (Freon-113), or in Freon-113/aqueous hybrid systems. Such processes require the use of large quantities of water, chlorofluorocarbons (CFCs) (for non-aqueous polymerizations), and fluorinated surfactants for emulsion polymerization. Many of the fluorinated surfactants typically employed in aqueous emulsion and suspension polymerizations are currently under scrutiny due to bioaccumulation and environmental persistence. These issues are collectively pointing towards the transition from the conventional fluoropolymer synthesis platforms to alternatives that meet the requirements of emerging public and regulatory demands (1).

Supercritical carbon dioxide ($scCO_2$) has become an attractive medium for polymerization processes because of its low toxicity, reasonably low cost, mild critical point ($T_c = 31.1^{\circ}C$, $P_c = 73.8$ bar), and its environmentally benign nature (2, 3). Another advantage is that the polymer can be synthesized and easily isolated in a dry and pure form (4). Many polymers have been synthesized in $scCO_2$, including fluoropolymers, polysiloxanes, poly(methyl methacrylate), polystyrene, and polycarbonates, as reviewed elsewhere (5–8). Unfortunately, besides fluoropolymers and polysiloxanes, most high molecular weight polymers do not show appreciable solubility in $scCO_2$, thus reducing the applications of homogeneous polymerization to a few materials (9–19). Most commercially available fluoropolymers are prepared from a relatively small group of olefins including tetrafluoroethylene (TFE), chlorotrifluoroethylene (CTFE), vinylidene fluoride (VDF), hexafluoropropylene (HFP), ethylene, and perfluoroalkyl vinyl ethers (PAVEs). Many of these monomers are flammable and some are explosive (1).

Tetrafluoroethylene (TFE) based copolymers have become premium high performance materials for a broad range of applications (1). These materials have been synthesized in non-aqueous solvents to avoid some of the problems associated with the use of water as solvent, such as the increased occurrence of carboxylic end groups. Further advantages may exist in the storage of TFE with CO_2, and many dangers can be avoided, such as autopolymerization (20). Baradie and Shoichet (21)

[†]On research leave from UNAM.
Address correspondence to: Eduardo Vivaldo-Lima, Departamento de Ingeniería Química, Facultad de Química, Universidad Nacional Autónoma de México (UNAM), 04510, México D.F., México. Fax: +(5255)-5622-5355; E-mail: vivaldo@servidor.unam.mx

reported the first synthesis of a series of fluorocarbon-VAc copolymers in $scCO_2$ in a surfactant free polymerization.

The literature on polymer chemistry in $scCO_2$ is extensive and keeps growing, as evidenced from the review by Kendall et al. (5). However, the modeling of polymerization processes in fluids at supercritical conditions has remained behind in research intensity. To the best of our knowledge, the first paper that reports the modeling of a free-radical heterogeneous homopolymerization in $scCO_2$ comes from the group of DeSimone (22), who modeled a heterogeneous process (the precipitation homopolymerization of VDF) as homogeneous. The groups of Kiparissides (23) and Morbidelli (24) have modeled the dispersion homopolymerization of MMA in $scCO_2$. The group of Morbidelli (25) has also modeled the homopolymerization of VDF as a heterogeneous process, being able to describe the bimodal molecular weight distribution. The modeling of dispersion copolymerization with crosslinking of vinyl/divinyl monomers in $scCO_2$ has been addressed by our own group (26).

The first commercial process for polymer production using a $scCO_2$ technology is related to the homogeneous/precipitation polymerization of fluoromonomers. New types of Teflon® products with enhanced performance and processing capabilities are being manufactured at the Fayetteville, North Carolina, plant of DuPont, in a USD 40 million facility that started up in late 2000 (27). Although the precipitation polymerization of VDF has been addressed in the open literature, considering the process as either homogeneous (22) (with fairly good results) or heterogeneous (25) (the true nature of the process), the modeling of the polymerization of other important fluoromonomers (proceeding as either homogeneous or precipitation processes) has not been reported.

The modeling of homogeneous homo- and copolymerizations of fluoromonomers in supercritical carbon dioxide is addressed in this paper. The homopolymerization of dihydroperfluorooctyl acrylate (FOA) (true homogeneous process) and the copolymerization of tetrafluoroethylene (TFE) with vinyl acetate (VAc) (surfactant-free precipitation process with enhanced solubility of the copolymer by the presence of TFE) in supercritical carbon dioxide are used as case studies. In the first case, the model would be specific for the system. In the second case, the model would be an approximation, since the copolymerization of TFE/VAc is not completely homogeneous. These polymerizations are modeled as simplified cases of the comprehensive mathematical model for vinyl/divinyl copolymerization in $scCO_2$ recently presented by our group (26). Model simulations are compared against limited experimental data on polymerization kinetics of these monomers in $scCO_2$ available in the literature.

2 Experimental

Although the focus of this paper is on the modeling of homogeneous homo- and copolymerizations of fluoromonomers in $scCO_2$, the simulated results were compared against experimental data (9, 21) from the literature.

The polymerization of FOA in $scCO_2$ at the same conditions reported by DeSimone et al. (9) ($T = 59.4^{\circ}C$, $P = 207$ bar, $m_{FOA} = 5$ g, $m_{AIBN} = 50$ mg, and the needed amount of CO_2 to fill the 10 mL reactor used in their experiments) was used as the first homogeneous homopolymerization case study.

The copolymerization of TFE and VAc in $scCO_2$ at the conditions reported by Baradie and Shoichet (21) ($T = 45^{\circ}C$, $P = 200$ bar, $m_{TFE} + m_{VAc} = 20$ g, and the needed amount of CO_2 to fill the 50 mL reactor used in their experiments) was used as the second case study for a surfactant-free precipitation polymerization, approximated as a homogeneous process.

3 Modeling

3.1 Reaction Scheme

The chemical system studied in this paper is the free radical homopolymerization and copolymerization of fluorinated monomers in $scCO_2$. The reaction scheme for a binary free-radical copolymerization is summarized in Table 1, as a simplified version of the copolymerization of vinyl/divinyl monomers previously addressed by our group (26, 28). In

Table 1. Reaction mechanism for binary free-radical copolymerization

Initiation	$I \xrightarrow{k_d} 2R^*_{in}$
	$R^*_{in} + M_1 \xrightarrow{k_1} R^\bullet_{1,0,1}$
	$R^*_{in} + M_2 \xrightarrow{k_2} R^\bullet_{0,1,2}$
Inhibition	$R^\bullet_{m,n,1} + Z \xrightarrow{k_{z1}} P_{m,n}$
	$R^\bullet_{m,n,2} + Z \xrightarrow{k_{z2}} P_{m,n}$
Propagation	$R^\bullet_{m,n,1} + M_1 \xrightarrow{k_{11}} R^\bullet_{m+1,n,1}$
	$R^\bullet_{m,n,1} + M_2 \xrightarrow{k_{12}} R^\bullet_{m,n+1,2}$
	$R^\bullet_{m,n,2} + M_1 \xrightarrow{k_{21}} R^\bullet_{m+1,n,1}$
	$R^\bullet_{m,n,2} + M_2 \xrightarrow{k_{22}} R^\bullet_{m,n+1,2}$
Transfer to monomer	$R^\bullet_{m,n,1} + M_1 \xrightarrow{kf_{11}} P_{m,n} + R^\bullet_{1,0,1}$
	$R^\bullet_{m,n,1} + M_2 \xrightarrow{kf_{12}} P_{m,n} + R^\bullet_{0,1,2}$
	$R^\bullet_{m,n,2} + M_1 \xrightarrow{kf_{21}} P_{m,n} + R^\bullet_{1,0,1}$
	$R^\bullet_{m,n,2} + M_2 \xrightarrow{kf_{22}} P_{m,n} + R^\bullet_{0,1,2}$
Transfer to small molecules (either solvent or transfer agent)	$R^\bullet_{m,n,1} + T \xrightarrow{kft_1} P_{m,n} + T^*$
	$R^\bullet_{m,n,2} + T \xrightarrow{kft_2} P_{m,n} + T^*$
Transfer to polymer	$R^\bullet_{m,n,1} + P_{r,s} \xrightarrow{kfp_1} P_{m,n} + R^\bullet_{r,s,1}$
	$R^\bullet_{m,n,2} + P_{r,s} \xrightarrow{kfp_2} P_{m,n} + R^\bullet_{r,s,2}$
Termination by disproportionation	$R^\bullet_{m,n,1} + R^\bullet_{r,s,1} \xrightarrow{ktd_{11}} P_{m,n} + P_{r,s}$
	$R^\bullet_{m,n,1} + R^\bullet_{r,s,2} \xrightarrow{ktd_{12}} P_{m,n} + P_{r,s}$
	$R^\bullet_{m,n,2} + R^\bullet_{r,s,1} \xrightarrow{ktd_{21}} P_{m,n} + P_{r,s}$
	$R^\bullet_{m,n,2} + R^\bullet_{r,s,2} \xrightarrow{ktd_{22}} P_{m,n} + P_{r,s}$
Termination by combination	$R^\bullet_{m,n,1} + R^\bullet_{r,s,1} \xrightarrow{ktd_{11}} P_{m+r,n+s}$
	$R^\bullet_{m,n,1} + R^\bullet_{r,s,2} \xrightarrow{ktc_{12}} P_{m+r,n+s}$
	$R^\bullet_{m,n,2} + R^\bullet_{r,s,1} \xrightarrow{ktc_{21}} P_{m+r,n+s}$
	$R^\bullet_{m,n,2} + R^\bullet_{r,s,2} \xrightarrow{ktc_{22}} P_{m+r,n+s}$

Table 2. Reaction mechanism for the free-radical homopolymerization

Initiation	$I \xrightarrow{k_d} 2I^\bullet$
	$I^\bullet + M \xrightarrow{k_i} R_1^\bullet$
Propagation	$R_x^\bullet + M \xrightarrow{k_p} R_{x+1}^\bullet$
Transfer to monomer	$R_x^\bullet + M \xrightarrow{k_{fm}} P_x + R_1^\bullet$
Transfer to polymer	$R_x^\bullet + P_y \xrightarrow{k_{fp}} P_x + R_y^\bullet$
Termination by disproportionation	$R_x^\bullet + R_y^\bullet \xrightarrow{k_{td}} P_x + P_y$
Termination by combination	$R_x^\bullet + R_y^\bullet \xrightarrow{k_{tc}} P_{x+y}$

the reaction mechanism of Table 1, the propagation through pendant double bonds reactions studied previously (26, 28) (crosslinking leading to "x" type—short length—linkages) have been removed, since no divinyl monomers are studied in this paper. If there is no comonomer present in the system, the reaction mechanism reduces to a conventional free radical homopolymerization (shown in Table 2). Symbols used in all Tables are defined in the nomenclature section of this paper.

3.2 Kinetic Model Equations

Tables 3 to 5 show the main aspects of the model used in this paper, including the kinetic and moment equations (Table 3), the free volume equations for diffusion-controlled phenomena (Table 4), and the definition of the pseudo-kinetic rate constants (Table 5). The development of the model for vinyl/divinyl copolymerization (26, 28) from which the simplified equations shown in Tables 3 to 5 were obtained, is based on the Tobita-Hamielec model (29, 30), different versions of which have been documented in detail elsewhere (26, 28, 31). It should be emphasized that the simplified form of the model for

Table 4. Diffusion-controlled equations used in binary free-radical copolymerization

Reaction	Difussion-controlled expression
Initiator efficiency	$f = f_0\, e^{-D(\frac{1}{V_f}-\frac{1}{V_{f0}})}$
Propagation	$k_{p_{ij}} = k^o_{p_{ij}}\, e^{-B(\frac{1}{V_f}-\frac{1}{V_{f\,cr2}})}$
Translational termination	$\overline{k}_{tcnij} = k^o_{tcn_{ij}}\, e^{-[A(\frac{1}{V_f}-\frac{1}{V_{f0}})]} + k_{tcrd}$
	$\overline{k}_{tcwij} = k^o_{tcw_{ij}} \left[\frac{\overline{P}_n}{\overline{P}_w}\right]^{\frac{x}{2}} e^{-[A(\frac{1}{V_f}-\frac{1}{V_{f0}})]} + k_{tcrd}$
Reaction-diffusion termination	$k_{tcrd} = C^o_{rd} k_{p_{pse}}(1-x)$
Fractional free-volume	$V_f = \sum_{i=1}^{N}[0.025 + \alpha_i(T - T_{g_i})\frac{V_i}{V_t}]$ i = monomer 1, monomer 2, polymer, solvent, CTA

Table 3. Kinetic and moment equations for binary free-radical copolymerization

Initiation	$\frac{d(V[I])}{Vdt} = -k_d[I]$
Overall conversion	$\frac{dx}{dt} = (k_p + k_{fm})(1-x)[R^\bullet]$
Moment equations for polymer radicals	$\frac{d(VY_0)}{Vdt} = 2fk_d[I] - (\overline{k}_{tcn} + \overline{k}_{td})\, Y_0^2$
	$\frac{d(VY_1)}{Vdt} = 2fk_d[I] + (k_{fm}[M] + k_{fT}[T]) + k_p[M]\, Y_0$ $-\{k_{fm}[M] + k_{fT}[T] + (\overline{k}_{tcn} + \overline{k}_{td})\, Y_0 + k_{fp}([Y_1 + Q_1] - Y_1)\}\, Y_1$
Moment equations for total polymer concentration	$\frac{d(V[Y_0 + Q_0])}{Vdt} = 2fk_d[I] + (k_{fm}[M] + k_{fT}[T])\, Y_0 - \frac{1}{2}\overline{k}_{tcn}\, Y_0^2$
	$\frac{d(V[Y_1 + Q_1])}{Vdt} = 2fk_d[I] + (k_{fm}[M] + k_{fT}[T])\, Y_0 + k_p[M]\, Y_0$
	$\frac{d(V[Y_2 + Q_2])}{Vdt} = 2fk_d[I] + (k_{fm}[M] + k_{fT}[T])\, Y_0 + k_p[M]\, Y_0$ $+2\,k_p[M]\, Y_1 + \overline{k}_{tcw}\, Y_1^2$
Divinyl monomer consumption	$\frac{df_2}{dt} = \left(\frac{f_2 - F_2}{1-x}\right)\frac{dx}{dt}$
Accumulated copolymer composition	$\overline{F_2} = \frac{f_{20} - f_2(1-x)}{x}$
Transfer to small molecule	$\frac{d(V[T]_i)}{Vdt} = -k_{fTi}[T_i][R^\bullet]$

Table 5. Pseudo-kinetic rate constants (pseudo-homopolymer approach) for binary free-radical copolymerization

Reaction	Pseudo-kinetic rate constant
Propagation	$k_p = \sum_{i=1}^{3}\sum_{j=1}^{2} k_{ij}\,\phi_i^{\bullet} f_j$
Inhibition	$k_z = \sum_{i=1}^{3} k_{zi}\,\phi_i^{\bullet}$
Transfer to monomer	$k_{fm} = \sum_{i=1}^{3}\sum_{j=1}^{2} k_{fm_{ij}}\,\phi_i^{\bullet} f_j$
Transfer to a small molecule	$k_{fT} = \sum_{i=1}^{3} k_{fT_i}\,\phi_i^{\bullet}$
Transfer to polymer	$k_{fp} = \sum_{i=1}^{3}\sum_{j=1}^{2} k_{fp_{ij}}\,\phi_i^{\bullet}\,\overline{F}_j$
Transfer to initiator	$k_{fI} = \sum_{i=1}^{3} k_{fI_i}\,\phi_i^{\bullet}$
Termination by disproportionation	$k_{td} = \sum_{i=1}^{3}\sum_{j=1}^{3} k_{td\,ij}\,\phi_i^{\bullet}\,\phi_j^{\bullet}$
Termination by combination	$k_{tc} = \sum_{i=1}^{3}\sum_{j=1}^{3} k_{tc\,ij}\,\phi_i^{\bullet}\,\phi_j^{\bullet}$

copolymerization of vinyl/divinyl monomers obtained in this paper when crosslinking is suppressed (namely, the case of vinyl/vinyl copolymerization), is equivalent to the well known models for multicomponet polymerization based on the pseudo-kinetic rate constants method (32–34), or the pseudo-homopolymer approach (35). The parameters used for the calculations presented in this paper are summarized in Tables 6 and 7. The model equations were solved using a self-developed Fortran code (26, 28).

4 Results and Discussion

4.1 Source of Model Parameters

All the parameters used in our calculations were taken from the literature, although the polymerization kinetics of these monomers has not been studied as extensively as other styrenic, methacrylic and acrylic monomers. The numerical values of the parameters used in this paper are listed in Table 6 for the case of FOA homopolymerization, and in Table 7 for the case of copolymerization of TFE/VAc. The model was tested by comparing the predicted profiles with experimental data of total monomer conversion, molecular weight development, and copolymer composition, in the case of copolymerization. For the homopolymerization of FOA only experimental data of molecular weight after 48 h of reaction (65% monomer conversion) were available (9).

Table 7. Kinetic parameters for the free-radical copolymerization of TFE/VAc in $scCO_2$

Parameter	Value	Reference
f_0, dimensionless	0.7	(10)
k_d, s^{-1}	$k_d = 1.053 \times 10^{15} \exp\left(-\frac{30660}{RT}\right)$	(28)
k_{11} L mol^{-1} s^{-1}	3258	(37)
k_{22} L mol^{-1} s^{-1}	2968	(36)
k_{ft}, L mol^{-1} s^{-1}	0.18 k_{11}	(28)
k_{fm}, L mol^{-1} s^{-1}	$k_{fm} = 2.31 \times 10^{6} \exp\left(-\frac{12671}{RT}\right)$	(28)
k_{fp}, L mol^{-1} s^{-1}	0.0	(28)
k_t, L mol^{-1} s^{-1}	5.8×10^{9}	(36)
k_{ft1}, k_{ft2}, L mol^{-1} s^{-1}	0.0133 k_{11}	(28)
r_1, dimensionless	$\left(\frac{k_{11}}{k_{12}}\right) = 1.03$	(21)
r_2, dimensionless	$\left(\frac{k_{22}}{k_{21}}\right) = 0.051$	(21)

4.2 Homogeneous Homopolymerization

The first case analyzed was the homogeneous homopolymerization of dihydroperfluorooctyl acrylate (FOA) in supercritical carbon dioxide at the same conditions reported by DeSimone et al. (9). Once the model was implemented, parameter sensitivity analyses were carried out. The first objective was to test the model implementation, namely, to verify that the expected trends were predicted by the model. The second objective of these sensitivity analyses was to determine

Table 6. Physical and kinetic parameters for the free-radical homopolymerization of FOA in $scCO_2$

Parameter, Units	Value, Case 1	Value, Case 2	Value, Case 3	Reference
k_p, L mol^{-1} s^{-1}	7400[a]	7400[a]	2960[b]	(38)
k_d, s^{-1}	3.4×10^{-6}	3.4×10^{-6}	3.4×10^{-6}	(9)
k_{fm}, L mol^{-1} s^{-1}	1.14×10^{-2}	1.14×10^{-2}	1.14×10^{-2}	(26)
k_t, L mol^{-1} s^{-1}	1.8×10^{8}[c]	740[d]	740[d]	(26, 38)
f	0.83	0.83	0.83	(9)

[a] k_p for TFE at 40°C.
[b] k_p for TFE at 40°C, corrected for pressure (taken as 40% of the value at normal conditions).
[c] k_t for styrene.
[d] Value for TFE at 40°C, corrected for pressure (taken as ten times the value at normal conditions).

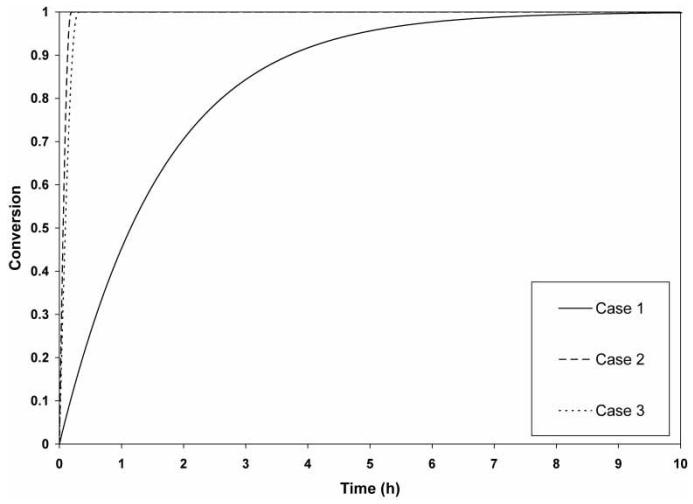

Fig. 1. Effect of k_p and k_t on polymerization rate for FOA polymerization in scCO$_2$, at P = 207 bar and T = 59.4°C.

bounds on the values of the propagation and termination kinetic rate constants, k_p and k_t, respectively, in case it was necessary to use them as fitting parameters to the experimental data from the literature that we had available.

Figures 1 and 2 show some of the most meaningful simulations of conversion vs. time and number and weigh average molecular weights vs. conversion, respectively, from these parameter sensitivity analyses studies. The values of k_p and k_t used in these simulations, shown in Table 6, were the corresponding values for TFE polymerization, since we could not find information about these kinetic rate constants for FOA in the open literature, and

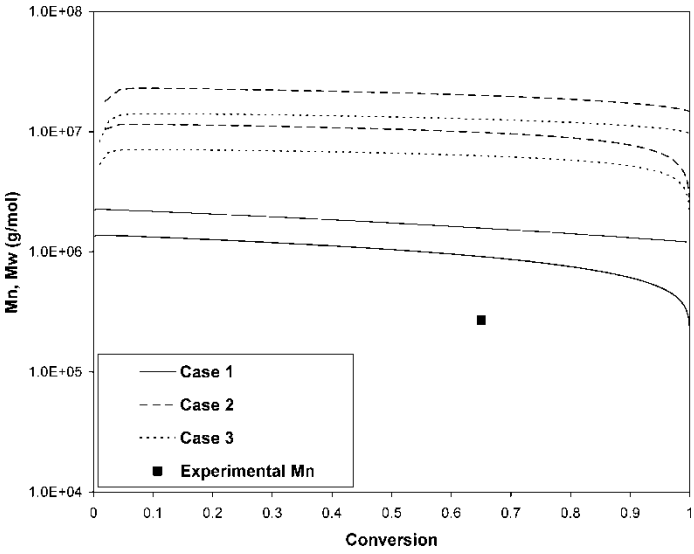

Fig. 2. Effect of k_p and k_t on molecular weight development (M_n and M_w) for FOA polymerization in scCO$_2$, at P = 207 bar and T = 60°C. The experimental value of M_n at 65% monomer conversion was taken from DeSimone et al. (9).

the fact that TFE and FOA are both fluorinated monomers. Case 1 was a simulation using the value of k_p for TFE polymerization at 40°C and 1 bar, and the value of k_t of styrene at the polymerization conditions simulated for FOA. In Case 2 the same k_p as in Case 1 was used, but the value of k_t was the one for TFE at 40°C, corrected for pressure (assuming that the value at high pressure was roughly ten times the value at 1 bar, as in the case of styrene (39)). Case 3 was a simulation using both the k_p and k_t of FOA polymerization at 40°C, but corrected for pressure assuming activation volumes and solvent effects similar to those of other vinyl monomers in scCO$_2$ (39). In all the cases simulated, the inclusion of diffusion-controlled effects did not significantly modify the produced profiles of polymerization rate and molecular weight development, a situation typical of solution polymerizations, given the very large contribution from the solvent to the available free volume.

The profiles of conversion vs. time shown in Figure 1 are very much in agreement with what would be expected, given the values of k_p and k_t used for the simulations. Case 1 corresponded to fairly fast propagating chains (large k_p), but with a fairly large k_t, thus producing a rather slow polymerization (given the inverse effect of k_t on the polymer radical concentration). The value of k_t used in cases 2 and 3 was very low, compared to the values typical in the polymerizations of styrene or other typical vinyl monomers, thus producing much higher concentrations of polymer radicals than those of case 1 and, consequently, a much faster polymerization rate. The three profiles produced polymerization rates much faster than what was observed experimentally. DeSimone et al. (9) reported 65% monomer conversion (not shown in Figure 1) at 48 h of polymerization time. In Figure 1, the reaction is completed to full conversion in less than 10 h, for the slowest set of conditions (Case 1).

Figure 2 shows the simulations of number and weight average molecular weights, M_n and M_w, vs. conversion for cases 1, 2 and 3 (see Table 6). For every set of curves identified with the same line, the lower one corresponds to M_n, and the upper one to M_w. Once again, the obtained results are in agreement with what was expected from typical free-radical polymerization trends. The case with the highest termination rate (Case 1) produces polymer with the shortest chain length (lowest molecular weight). From the two cases with the same value of k_t, the one with the higher k_p (Case 2) produces polymer with higher molecular weight. Also shown in Figure 2 is an experimental measurement of M_n for this polymerization system. The reported value was obtained at 48 h of polymerization time, which corresponded to 65% monomer conversion (9). The best approximation to the experimental value of M_n was the one obtained with the parameters used for Case 1. The predicted value of M_n at 65% monomer conversion (Case 1) was significantly higher than the measured value. It is unfortunate that no more experimental data was available in the open literature.

4.3 Copolymerization of TFE and VAc

The second case study modeled was the surfactant-free precipitation copolymerization of TFE/VAc (approximated as homogeneous) in supercritical carbon dioxide. This is a reasonable assumption, since the copolymerization proceeds mostly in a single phase because the monomer acts as a cosolvent, enhancing the solubility of the produced polymer during the reaction (21). In that study, the initial composition of fluoromonomer was increased from 13.1 to 83.3%, on a molar basis, in five cases (13.1%, 34.5%, 50%, 67.7% and 83.3%). The five cases were simulated with our model, obtaining the profiles shown in Figures 3 to 6 for conversion vs. time, average molecular weights vs. conversion, polydispersity index (PDI) vs. conversion, and copolymer composition vs. conversion, respectively. In the simulations, monomer 1 was vinyl acetate, and TFE was monomer 2. Diffusion-controlled effects were neglected, since the copolymerization proceeded mostly as a solution polymerization process. In all the simulated cases, there was only one experimental point available per case analyzed. The experimental data were obtained after 24 h of polymerization (21).

Figure 3 shows the effect of the initial concentration of fluoromonomer, from 13.1 to 83.3 mol% of the total monomer mixture, on the rate of polymerization, expressed as total monomer conversion vs. time. It is observed that both the polymerization rate and the limiting conversion increase as the amount of monomer 2 (TFE) is increased. Since the homopolymerization propagation kinetic rate constants used (k_{11} and k_{22}), and the cross-propagation kinetic rate constant between a polymer radical with monomer 1 in its end and monomer 2 are very much alike, the higher polymerization rates as monomer 2 is increased in the formulation observed in Figure 3 can be explained in terms of the reactivity ratio r_2, which is very low. The very low value of r_2 indicates that polymer radicals ending in monomer 2 are extremely reactive towards monomer 1. The net effect is that the overall polymerization rate is increased. The effect of the limiting monomer conversion increasing as the amount of TFE is increased, clearly shown in the simulations of Figure 3, was also obtained experimentally by Baradie and Shoichet (21), although the range of limiting conversion values was different. In the simulations, the limiting conversion values go from 84 to 99% when f_{TFE} goes from 13.1 to 83.3%, whereas the range obtained experimentally (at 48 hours of reaction time) (21) was from 75 to 83% limiting monomer conversion. One possible explanation for this discrepancy is that the value of k_{22} used in our simulations was for TFE at 60°C (at the correct pressure), and the temperature of the simulated copolymerization was only 45°C. The true value of k_{22} should have been significantly lower, thus likely producing lower polymerization rates, and lower limiting conversions.

Figure 4 shows the effect of the initial amount of TFE on the molecular weight development, namely, on M_n and M_w. It is observed that there are pairs of profiles identified with the same type of line. In each pair, the lower profile corresponds to M_n, and the upper one to M_w. Considering that k_t was assumed constant and independent of the monomer unit at the end of each polymer radical (an assumption given by the value of k_t used, and not necessarily a model limitation), the different values of M_n and M_w obtained are caused by the different overall values of k_p (propagation pseudo-kinetic rate constant). As explained before, the fact that polymer radicals ended in TFE monomer units are extremely reactive with VAc (because of the very low value of r_2) causes the polymer molecules to grow faster, reaching higher molecular weights when the amount of TFE is increased. It is also observed in Figure 4 that the ideal solution polymerization behavior (molecular weight progressively decreasing as polymerization proceeds, showing almost constant values of M_n and M_w) is observed up to about 80% monomer conversion. After 85% monomer conversion, the profiles of M_n seem to overlap and

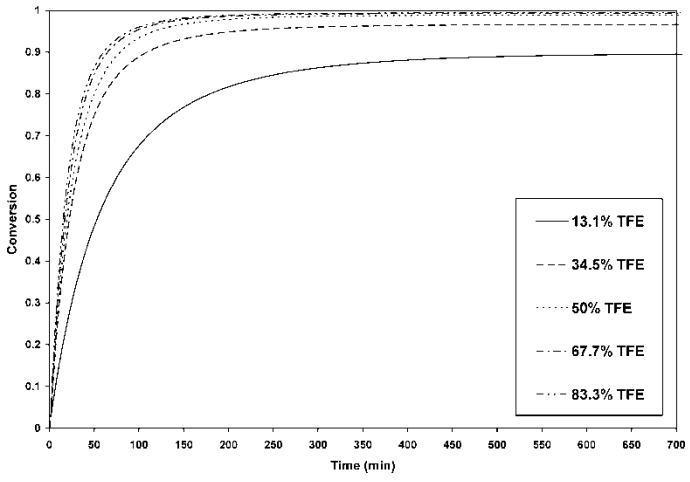

Fig. 3. Effect of initial fluoromonomer composition on polymerization rate in the copolymerization of TFE and VAc at the experimental conditions of Baradie and Shoichet (21).

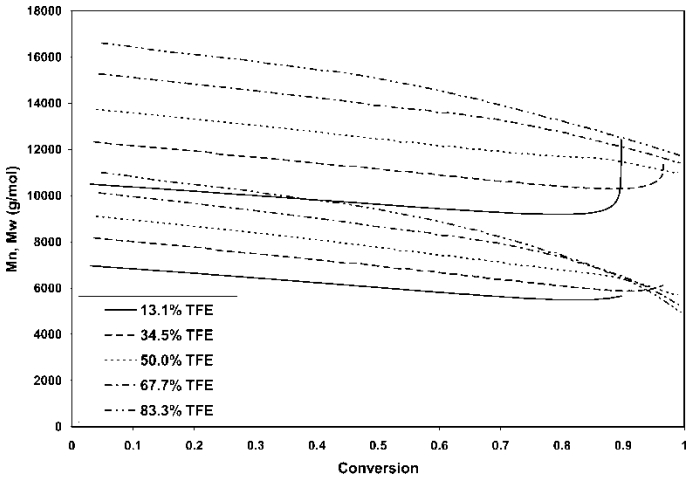

Fig. 4. Effect of initial fluoromonomer composition on molecular weight development (M_n and M_w) in the copolymerization of TFE and VAc at the experimental conditions of Baradie and Shoichet (21).

then the behavior reverses, whereas the M_w profiles seem to approach each other, but do not overlap. This behavior may be attributed to very moderate diffusion-controlled effects when the polymerization is very close to completion. It should be emphasized that the calculations with low content of TFE (13.1 and 34.5%) were carried out with the diffusion-controlled equations activated. The experimental values of M_n reported by Baradie and Shoichet (21) (not shown in the plot) showed the same trends predicted with the model (M_n at high conversions increasing with the initial amount of TFE), but the numerical values were almost one order of magnitude higher that the predicted ones. Once again, the fact of using a high value of k_p (a value of k_{22} valid at 60°C, instead of 45°C) produced very fast polymerization rates (Figure 3) and low number average molecular weights.

The effect of TFE content on molecular weight development is further illustrated in Figure 5 as polydispersity index (PDI) vs. conversion. It is observed that PDI increases slowly as the polymerization proceeds, but there is no difference among the five profiles up to about 60% monomer conversion. Thereafter, the polydispersity increases as the initial amount of TFE is increased. Only the profile at 13.1% TFE shows a different behavior, as in the previous cases, since PDI is predicted to increase steadily at about 89% monomer conversion. As explained before, this behavior could be attributed to not disconnecting the diffusion-controlled calculations in that case and in the one at 34.5% of TFE. The increasing trend on PDI as the initial amount of TFE is increased can be rationalized in terms of the higher reactivity of polymer radicals ended in TFE towards VAc. The high reactivity of TFE may promote obtaining many short chains, and when it is completely consumed, the amount of polymer radicals ended in TFE may decrease, and the chain length of the polymer molecules produced at the later stages of the polymerization might be larger, thus producing a more heterogeneous distribution, with higher PDI values.

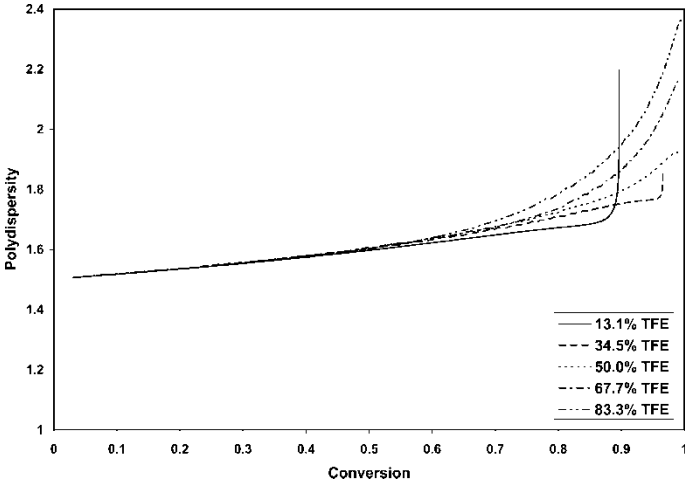

Fig. 5. Effect of initial fluoromonomer composition on polydispersity index (PDI) in the copolymerization of TFE and VAc at the experimental conditions of Baradie and Shoichet (21).

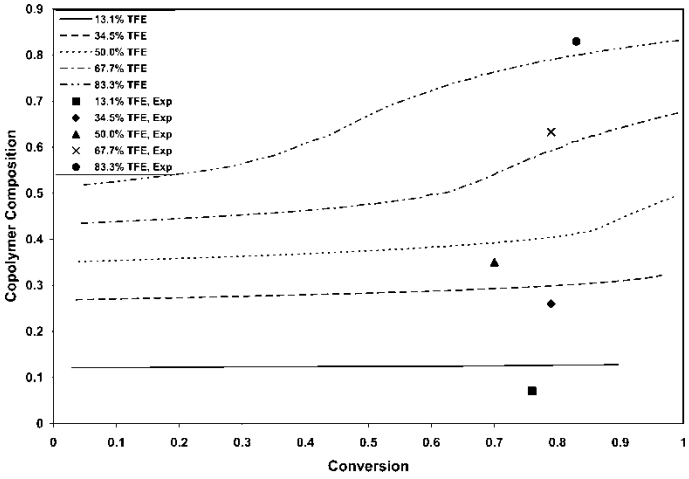

Fig. 6. Effect of initial fluoromonomer composition on copolymer composition in the copolymerization of TFE and VAc at the experimental conditions of Baradie and Shoichet (21). Experimental data from the same reference (21).

The experimental values of PDI measured by Baradie and Shoichet (21) span over the same range of PDI observed in Figure 5 (from 1.62 to 2.14), but these values were obtained in a conversion range from 70 to 83% monomer conversion, whereas this range is obtained with our model at a later conversion range (at about 95% monomer conversion).

The last feature of the copolymerization of TFE and VAc studied in this paper was the copolymer composition of the polymer product, expressed as the mole fraction of TFE incorporated into the copolymer. As expected, when the amount of TFE is increased, the content of TFE in the copolymer is also increased, as observed in Figure 6. There is good agreement between the predicted profiles calculated with our model and the measured experimental data reported by Baradie and Shoichet (21) at 24 h of polymerization time. This result is an indication that although the individual values of k_{11} and k_{22} may be overestimated (according to the analyses of Figures 3 to 5), the reactivity ratios, which ultimately determine the copolymer composition of the produced polymer, are good enough for this copolymerization system.

5 Conclusions

The homogeneous homopolymerization of FOA and the copolymerization of TFE and VAc (approximated as homogeneous) in carbon dioxide at supercritical conditions were addressed in this paper. The model used can be considered as "standard" in the polymer reaction engineering community, but the specific polymerization systems had not been previously modeled.

The main limitation for the modeling of homogeneous polymerization of fluoromonomers in scCO$_2$ is the lack of reliable kinetic rate constants, and the availability in the open literature of only a few experimental kinetic studies

which can be used for parameter estimation purposes. The qualitative behavior of the system was well described, which is certainly not surprising, since the solution copolymerization of vinyl monomers is a well understood process in the polymer reaction engineering field. Even when the parameters used were only approximate to the actual system, the agreement between model predicted profiles and the limited available experimental data was reasonably good.

6 Nomenclature

A	Effectiveness factor to account for overlap of free volume and separation of reactive radicals
B	Effectiveness factor to account for overlap of free volume and separation of monomer/polymer radicals
C^o_{rd}	Proportionality factor for reaction-diffusion termination constant, L mol^{-1}
D	Effectiveness factor to account for overlap of free volume and separation of fragment radical molecules
f	Initiator efficiency
f_0	Initial initiator efficiency
f_1	Relative vinyl monomer concentration (mol fraction)
f_2	Relative divinyl monomer concentration (mol fraction)
F_2	Instantaneous relative composition of monomer 2 in polymer
$\overline{F}_2$	Accumulated copolymer composition (molar relative content of DVB in copolymer)
f_{20}	Initial divinyl monomer concentration
F_2	Instantaneous relative composition of monomer 2 in polymer
K	Solubility constant of solvent (carbon dioxide) in monomer mixture
k_d	Initiator decomposition kinetic rate constant, s^{-1}
k_{fm}	Pseudo-kinetic rate constant for chain transfer to monomer, L mol^{-1} s^{-1}
k_{fp}	Pseudo-kinetic rate constant for chain transfer to polymer, L mol^{-1} s^{-1}
k_{fT}	Pseudo-kinetic rate constant for chain transfer to a small molecule, L mol^{-1} s^{-1}
k_{fz}	Pseudo-kinetic rate constant for chain transfer to a small molecule, L mol^{-1} s^{-1}
k_p	Pseudo-kinetic rate constant for propagation, L mol^{-1} s^{-1}
$\bar{k}_{pij}$	Effective propagation kinetic rate constant between radical type i with monomer j, L mol^{-1} s^{-1}
k^0_{pij}	Intrinsic chemical propagation kinetic rate constant for propagation, L mol^{-1} s^{-1}
k_{tc}	Pseudo kinetic rate constant for termination by combination, L mol^{-1} s^{-1}
$\bar{k}_{tc_{nij}}$	Effective number average termination by combination kinetic rate constant between radicals type i and j, L mol^{-1} s^{-1}
$\bar{k}_{tc_{wij}}$	Effective weight average termination by combination kinetic rate constant between radicals type i and j, L mol^{-1} s^{-1}
k^0_{tcnij}	Intrinsic chemical kinetic rate constant for number average termination by combination between radicals i and j, L mol^{-1} s^{-1}
k^0_{tcwij}	Intrinsic chemical kinetic rate constant for weight average termination by combination between radicals i and j, L mol^{-1} s^{-1}
$\bar{k}_{tcrd}$	Reaction diffusion termination kinetic constant, L mol^{-1} s^{-1}
k_{td}	Pseudo kinetic rate constant for termination by disproportionation, L mol^{-1} s^{-1}
k_z	Pseudo kinetic rate constant for inhibition, L mol^{-1} s^{-1}
M	Total monomer
M_1	Monomer 1
M_2	Monomer 2
M_1^*	Monomeric radicals of type 1
M_2^*	Monomeric radicals of type 2
$[M]$	Total monomer concentration, mol L^{-1}
M_n	Number average molecular weight
M_w	Weight average molecular weight
PDI	Polydispersity index
$P_{m,n}$	Polymer molecule with m units of monomer 1 and n units of monomer 2
$\overline{P}_n$	Number average chain length
$\overline{P}_w$	Weight average chain length
P_r	Dead polymer molecules wit chain length r
$[P_r]$	Concentration of polymer with chain length r, mol L^{-1}
Q_i	Moment i of the dead polymer distribution, mol L^{-1}
R	Universal gas constant, cal mol^{-1} K^{-1}
r_1	Reactivity ratio, monomer 1
r_2	Reactivity ratio, monomer 2
$[R_1^\bullet]$	Concentration of polymer radicals of size 1, mol L^{-1}
$[R^\bullet]$	Total concentration of polymer radicals, mol L^{-1}
$R^\bullet_{in}$	Primary radicals from initiator decomposition
$R^\bullet_{m,n,i}$	Polymer radicals with m units of monomer 1, n units of monomer 2, with active center located on monomer unit i
$R^\bullet_r$	Polymer radical of size r
$[T]$	Concentration of small molecules, mol L^{-1}
Tg_i	Glass transition temperature for species i, °C,
V	Total volume, liters
V_0	Total initial volume, liters
V	Volume, liters
V_i	Volume of species i, liters
V_f	Fractional free volume
V_{fcr2}	Critical fractional free volume for glassy effect

x General (overall) conversion
Y_i Moment i of the polymer radical distribution, mol L^{-1}
$[Z]$ Inhibitor concentration, mol L^{-1}

6.1 Greek Letters

α_i Expansion coefficient for species i, °C^{-1}
$\phi_i^{\bullet}$ Mol fraction of radicals of type i
ρ_{CO_2} Carbon dioxide density, g L^{-1}
ρ_a Crosslinking density

7 Acknowledgements

Financial support from the National Council for Science and Technology of Mexico (CONACyT) (Project IAMC U40259-Y and the Ph.D. scholarship to I.A. Q.-O.), and from UNAM (DGAPA Projects PAPIIT IN100702, IX115404, and IN104107 and the DGEP Ph.D. scholarship to I.A. Q.-O.) is gratefully acknowledged. I. A. Quintero-Ortega also acknowledges the financial support from the Department of Chemical Engineering of Auburn University, for her research stay at Auburn University as visiting scholar. E. Vivaldo-Lima acknowledges the financial support from DGAPA-UNAM (PASPA Program) and the Department of Chemical Engineering of the University of Waterloo for his research stay at the University of Waterloo. G. Luna-Bárcenas acknowledges support from NSF-CONACyT 39377-U and CONACyT 42728-Y.

8 References

1. Wood, C.D., Cooper, A.I. and DeSimone, J.M. (2004) *Curr. Opinion Solid State Mater. Sci.*, **8**, 325–331.
2. Eckert, C.A., Knutson, B.L. and Debenedetti, P.G. (1996) *Nature* (London), **373**, 313–318.
3. Leitner, W. (2000) *Nature* (London), **405**, 129–130.
4. Michel, U., Resnick, P., Kipp, B. and DeSimone, J.M. (2003) *Macromolecules*, **36**, 7107–7113.
5. Canelas, D.A. and DeSimone, J.M. (1997) *Adv. Polym. Sci.*, **133**, 103–140.
6. Kendall, J.L., Canelas, D.A., Young, J.L. and DeSimone, J.M. (1999) *Chem. Rev.*, **99**, 543–563.
7. Cooper, A.I. (2000) *J. Mater. Chem.*, **10**, 207–234.
8. Sarbu, T., Styranec, T. and Beckman, E.J. (2000) *Nature* (London), **405**, 165–168.
9. DeSimone, J.M., Guan, Z. and Elsbernd, C.S. (1992) *Science*, **257**, 945–947.
10. Guan, Z., Combes, J.R., Menceloglu, Y.Z. and DeSimone, J.M. (1993) *Macromolecules*, **26**, 2663–2669.
11. Combes, J.R., Guan, Z. and DeSimone, J.M. (1994) *Macromolecules*, **27**, 865–867.
12. Kapellen, K.K., Mistele, C.D. and DeSimone, J.M. (1996) *Macromolecules*, **29**, 495–496.
13. van Herk, A.M., Manders, B.G., Canelas, D.A., Quadir, M. and DeSimone, J.M. (1997) *Macromolecules*, **30**, 4780–4782.
14. DeSimone, J.M., Maury, E.E., Menceloglu, Y.Z., McClain, J.B., Romack, T.J. and Combes, J.R. (1994) *Science*, **265**, 356–359.
15. Christian, P., Giles, M.R., Griffiths, R.M.T., Irvine, D.J., Major, R.C. and Howdle, S.M. (2000) *Macromolecules*, **33**, 9222–9227.
16. Shiho, H. and DeSimone, J.M. (2001) *Macromolecules*, **34**, 1198–1203.
17. Li, G., Yates, M.Z., Johnston, K.P. and Howdle, S.M. (2000) *Macromolecules*, **33**, 4008–4014.
18. Giles, M.R., Griffiths, R.M.T., Aguiar-Ricardo, A. and Silva, M.M.C.G. (2001) *Macromolecules*, **34**, 20–25.
19. Fehrenbacher, U. and Ballauff, M. (2002) *Macromolecules*, **35**, 3653–3661.
20. Hougham, G., Cassidy, P.E., Johns, K. and Davidson, T. (1999) *Fluoropolymers 1: Synthesis*; Kluwer Academic/Plenum Publishers: New York, 191–205.
21. Baradie, B. and Shoichet, M.S. (2002) *Macromolecules*, **35**, 3569–3575.
22. Charpentier, P.A., Kennedy, K.A., DeSimone, J.M. and Roberts, G.W. (1999) *Macromolecules*, **32**, 5973–5975.
23. Chatzidoukas, C., Pladis, P. and Kiparissides, C. (2003) *Ind. Eng. Chem. Res.*, **42**, 743–751.
24. Mueller, P.A., Storti, G. and Morbidelli, M. (2005) *Chem. Eng. Sci.*, **60**, 377–397.
25. Mueller, P.A., Storti, G., Morbidelli, M., Apostolo, M. and Martin, R. (2005) *Macromolecules*, **38**, 7150–7163.
26. Quintero-Ortega, I.A., Vivaldo-Lima, E., Luna-Bárcenas, G., Alvarado, J.F.J., Louvier-Hernández, J.F. and Sanchez, I.C. (2005) *Ind. Eng. Chem. Res.*, **44**, 2823–2844.
27. Stone, D.L.H. Innovation. *Fluoropolymers Made with New Supercritical CO_2 Technology*; DuPont Corporate News, DuPont Magazine European Edition, Number 4, p. 4, 2002.
28. Vivaldo-Lima, E., Hamielec, A.E. and Wood, P.E. (1994) *Polym. React. Eng.*, **2**, 87–162.
29. Tobita, H. and Hamielec, A.E. Crosslinking kinetics in free-radical copolymerization. In *Polymer Reaction Engineering*; Reichert, K.-H. and Geiseler, W. (eds.); VCH Publishers: New York, 43–83, 1989.
30. Tobita, H. and Hamielec, A.E. (1989) *Macromolecules*, **22**, 3098–3105.
31. Vivaldo-Lima, E., Wood, P.E., Hamielec, A.E. and Penlidis, A. (1998) *J. Polym. Sci., Polym. Chem.*, **36**, 2081–2094.
32. Hamielec, A.E. and MacGregor, J.F. Modelling copolymerization-control of chain microstructure, long chain branching, crosslinking and molecular weight distributions. In *Polymer Reaction Engineering*; Reichter, K.H. and Geisler, W. (eds.); Hanser Publishers: New York, 21, 1983.
33. Hamielec, A.E. and Tobita, H. Polymerization processes. In *Ullmanńs Encyclopedia of Industrial Chemistry*; Wiley-VCH: Weinheim; Vol. A21, 305, 1992.
34. Dubé, M.A., Soares, J.B.P., Penlidis, A. and Hamielec, A.E. (1997) *Ind. Eng. Chem. Res.*, **36(4)**, 966–1015.
35. Saldívar, E., Dafniotis, P. and Ray, W.H. (1998) *J. Macromol. Sci. Rev. Macromol. Chem. Phys.*, **C38(2)**, 207–325.
36. Charpentier, P.A., DeSimone, J.M. and Roberts, G.W. (2000) *Ind. Eng. Chem. Res.*, **39**, 4588–4596.
37. Kovarskii, A.L. *High Pressure Chemistry and Physics of Polymers*; CRC Press Inc: USA238–239, 1994.
38. Kamachi, M. and Yamada, B. Propagation and termination constants in free radical polymerization. In *Polymer Handbook, 4th edition*; Brandrup, J., Immergut, E.H. and Grulke, E.A. (eds.); John Wiley and Sons Inc: New York, 1999.
39. Beuermann, S. and Buback, M. (2002) *Prog. Polym. Sci.*, **27(2)**, 191–254.